Assessing the Validity of Image-Based DVH Metrics for Y-90 Tare Dosimetry

W Siman, PhD[1,*], S C Kappadath, PhD[2]

Department of Radiology and Imaging Sciences

1. Emory University, Department of Radiology and Imaging Science, Atlanta GA USA 2. UT MD Anderson Cancer Center, Department of Imaging Physics, Houston TX USA
*correspondence: wsiman@emory.edu

TAKE-HOME MESSAGES

- ❑ **SPECT-like DVHs** largely collapsed toward **Dmean**, offering little added information beyond mean-dose reporting.
- ❑ **PET-like DVHs** remained imperfect, but may preserve **residual heterogeneity information** under selected conditions relevant to **Y-90 TARE personalization**.

INTRODUCTION

- ❑ Dose Volume Histogram (DVH) metrics such as D90 and D10 are increasingly reported in Y-90 TARE dosimetry.
- ❑ Unlike external beam radiation therapy, Y-90 DVHs are derived from **limited-resolution** PET or SPECT images.
- ❑ **When heterogeneity is not spatially resolved, D90 and D10 may become largely predictable from Dmean.** In that setting, DVH metrics may be calculable but not independently informative.
- ❑ **Aim:** Determine how tumor size, intratumoral heterogeneity, and image resolution affect the reliability of image-based D90 and D10 in Y-90 dosimetry.
- ❑ **Significance:** Define when D90 and D10 are true heterogeneity metrics versus resolution-limited surrogates of Dmean.

MATERIALS AND METHODS

- ❑ **Analytically defined 3D digital phantoms** were generated in Python to model tumor geometry and intratumoral heterogeneity under controlled conditions.
- ❑ Models included **uniform spheres**, **cold regions**, and **hot regions**, providing known ground truth for DVH analysis.
- ❑ **Y-90-like** reference **dose maps** were generated using a **3-mm Gaussian kernel**; broader FWHM kernels simulated **PET-** and **SPECT-like** image degradation.
- ❑ Dmean, D90, and D10 were extracted from each simulated dose map.
- ❑ **R^2** were used to quantify when D90 and D10 became redundant with Dmean.

KEY RESULTS AND SUMMARY

- ❑ DVHs were affected by **lesion size and effective resolution** even in uniform activity spheres.
- ❑ For spheres with cold cores, worsening resolution increased **D90 redundancy with Dmean**.
- ❑ For spheres with hot spots, worsening resolution increased **D10 redundancy with Dmean**.
- ❑ Image-based DVH metrics are most meaningful when the hot or cold regions they describe remain **spatially resolvable**.
- ❑ DVH interpretation in Y-90 dosimetry should account for **tumor size, heterogeneity scale, and effective image resolution**.

RESULTS AND DISCUSSION

1. Uniform Activity Spheres: DVH Depends on Lesion Size and Effective Resolution

- ❑ **DVH fidelity decreases** as lesion size approaches the effective imaging resolution.
- ❑ **PET-like resolution (5–10 mm)** largely preserves D90/Dmean trends for larger lesions, whereas **SPECT-like resolution (15–20 mm)** progressively obscures them.
- ❑ **Loss of monotonicity** between blurred and reference D90/Dmean indicates that the DVH metric has become **resolution-dominated** rather than reflective of the underlying dose distribution.

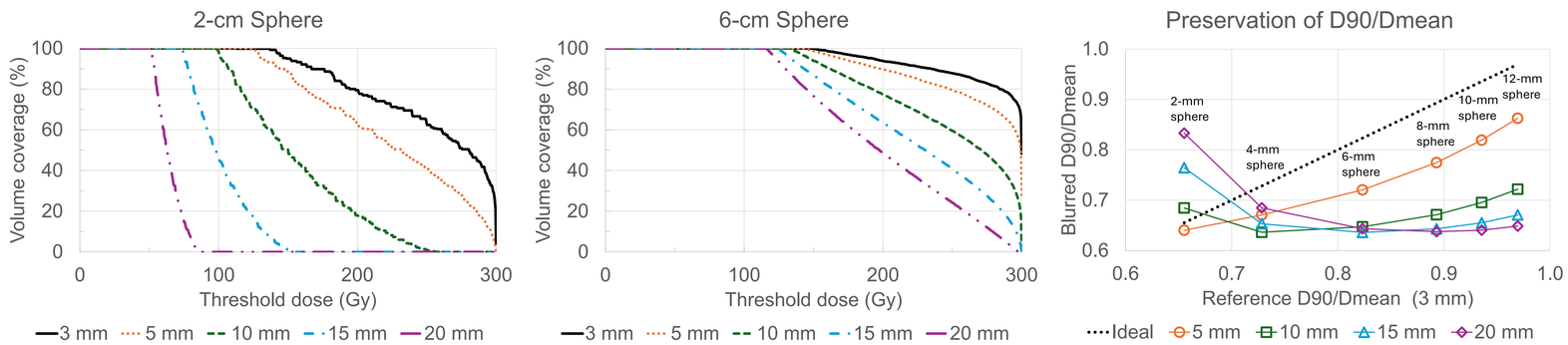

Figure 1. Effect of spatial resolution on DVH metrics in uniform spheres. Left/Center: DVHs for 2- and 6-cm spheres using 3-mm reference, 5–10 mm PET-like, and 15–20 mm SPECT-like Gaussian blurring. **Right:** Blurred D90/Dmean versus the corresponding 3-mm reference value for sphere diameters of 2–12 cm; the identity line indicates perfect agreement.

2. Spheres w/ Cold Spots: Spatial Blurring Makes D90 Increasingly Redundant with Dmean

- ❑ At the **3-mm reference resolution**, cold-spot geometry produced substantial variation in D90 among lesions with similar Dmean.
- ❑ This variability remained **appreciable** at **10-mm PET-like resolution**, but became **minimal** at **20-mm SPECT-like resolution**.
- ❑ Thus, worsening spatial resolution progressively converts D90 from a heterogeneity-sensitive metric into a predictable transformation of Dmean.

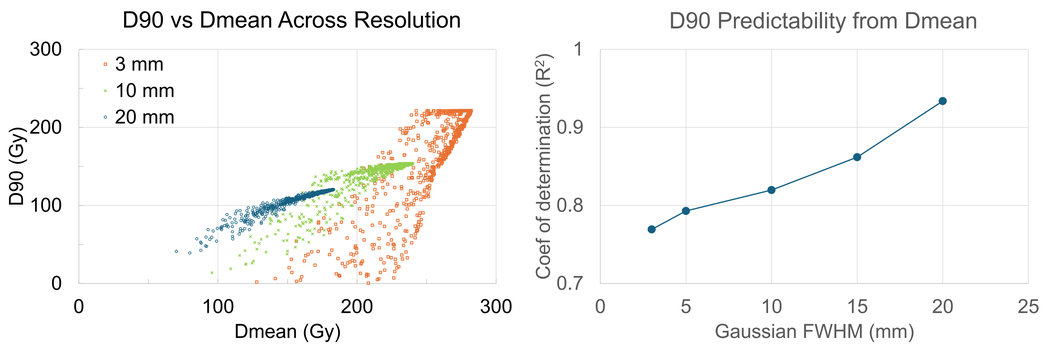

Figure 2. Spatial-resolution dependence of the Dmean–D90 relationship in cold-spot simulations. 1000 5-cm spheres contained a single randomly located cold spot with diameter 4–40 mm and relative uptake 0–1. **Left:** The broad Dmean–D90 spread at the 3-mm reference resolution narrowed progressively at 10 and 20 mm. **Right:** R^2 increased from 0.77 to 0.93, quantifying the increasing predictability of D90 from Dmean.

3. Spheres w/ Hot Spots: Spatial Blurring Makes D10 Increasingly Redundant with Dmean

- ❑ At the **3-mm reference resolution**, hotspot geometry produced substantial variation in **D10** among lesions with similar Dmean, indicating preserved high-dose heterogeneity information.
- ❑ This D10 variability **persisted** at **10-mm PET-like** resolution, but was largely **lost** at **20-mm SPECT-like** resolution.
- ❑ Thus, worsening spatial resolution progressively converts **D10** from a hotspot-sensitive DVH metric into a predictable transformation of Dmean.

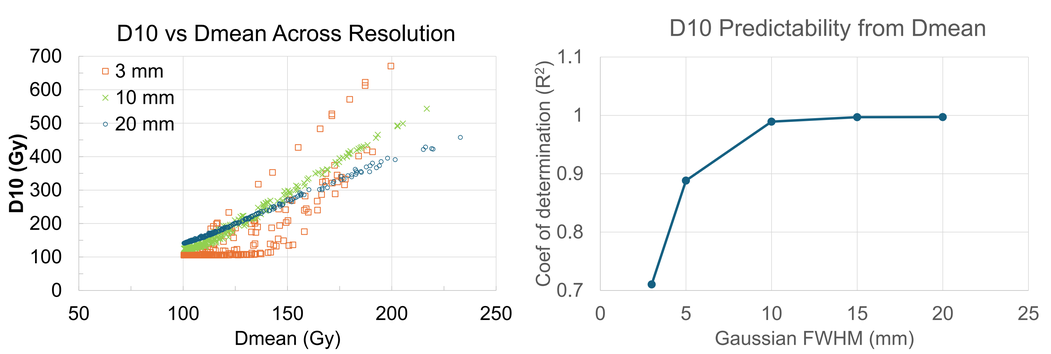

Figure 3. Spatial-resolution dependence of the Dmean–D10 relationship in hot-spot simulations. 300 5-cm spheres contained a single randomly located hotspot with radius 3–12 mm and relative uptake 2–10. **Left:** The broad Dmean–D10 spread at the 3-mm reference resolution narrowed progressively at 10 and 20 mm. **Right:** R^2 increased from 0.71 to ~1.00, quantifying the increasing predictability of D10 from Dmean.